Laser Photochemical Deposition of Gold from Trialkylphosphine Alkylgold(I) Complexes

Jack L. Davidson,[†] Phillip John,[†,*] Peter G. Roberts,[†] Michael G. Jubber,[‡] and John I. B. Wilson[‡]

Departments of Chemistry and Physics, Heriot-Watt University, Riccarton, Edinburgh EH14 4AS, UK

Received March 15, 1994. Revised Manuscript Received May 23, 1994[⊗]

The deposition of gold bearing tracks, by the argon ion laser photolysis at 257 nm of $R'Au^{I}PR_3$, $R,R' = C_2H_5$, CH_3, is reported. Deposits were obtained on optically polished fused quartz and (100) n-type single crystal silicon with a thermally grown oxide layer (3000 Å). Tracks were deposited at a range of scan speeds from 0 to 200 $\mu m\ s^{-1}$ and characterized by scanning electron microscopy (SEM), laser ionization mass analysis (LIMA), and scanning profilometry. Electrical resistivities as low as 4.51 $\mu\Omega$ cm, within a factor of 3 of the value for bulk gold (2.44 $\mu\Omega$ cm), were measured for tracks deposited at 40 mW and a scanning speed of 7.5 $\mu m\ s^{-1}$. However, the electrical conductivity of the deposits is highly sensitive to the structure of the organogold precursor. Mass spectral data obtained by LIMA indicate that the incorporation of the precursor and/or various photolysis byproducts into the deposit is related to the volatility of the ligand. Contamination is observed in tracks deposited from compounds containing the heavier ligand. Also, the electrical resistivities are correspondingly higher. Although isothermal annealing above 100 °C removes fragments containing the ligand, the resulting electrical conductivities are not improved.

Introduction

Metallization on both the micron[1] and submicron[2] scale can be achieved using laser-induced chemical vapor deposition. Pyrolytic "direct-writing" of discretionary patterns of gold, using a 514 nm argon ion laser, from the lower oxidation state trialkylphosphine alkylgold(I) precursors, $R'Au^{I}PR_3$, R, R' = C_2H_5, CH_3 produces high-purity tracks with electrical resistivities within a factor of 2 of the value for bulk gold.[3] Deposits with comparable resistivities have been obtained[4] at higher deposition rates from Au(III) precursors, e.g., dimethylgold(III) 2,4-pentanedionate, albeit with the inclusion of a postdeposition annealing step. Latterly, high-purity gold films exhibiting resistivities of 2.6 $\mu\Omega$ cm have been grown[5] by conventional chemical vapor deposition techniques from $R'Au^{I}PR_3$, R = CH_3, R' = C_2H_5. In addition, deposition occurred on atomically clean metallic surfaces below the decomposition temperature of the precursor with a high degree of selectivity over oxidised or nonmetallic surfaces.

In conjunction with the development of new photochemically labile precursors, photolytic laser deposition offers the prospect of interconnecting devices fabricated from thermally sensitive semiconductors. However, in common with other metals,[1] the photochemical deposition of gold[6] at lower temperatures produces deposits with significantly higher impurity levels. The resulting tracks exhibit poor electrical conductivities which cannot be improved by thermal annealing without adversely affecting the morphology and adhesion of the tracks. Progress in depositing pure metallic conductors at low temperatures requires a detailed knowledge of the photochemistry of the gas and adsorbed phases.[7] However, there is little information concerning the decomposition mechanisms of trialkylphosphine alkylgold(I) complexes in the gas phase. Studies of the mechanisms of their thermolysis[8] and photolysis[9] in the condensed phases have been limited to the triphenylphosphine derivatives. The liquid and solid phase thermolysis of $RAu^{I}PPh_3$, R = Me, Et, *i*-Pr, and *t*-Bu at 100 °C is limited by a rate determining primary dissociation step involving loss of a free phosphine ligand. Reductive coupling of RAu with the gold complex explains the nature and relative yields of the hydrocarbon products. The latter are not consistent with a free radical mechanism. In contrast, the UV photolysis of $MeAu^{I}PPh_3$ in $CDCl_3$ solution proceeds via intersystem crossing to the triplet state and thence formation of a methyl radical.

The micron-scale dimensions of laser-drawn tracks has restricted analyses to various scanning electron or

[†] Department of Chemistry.
[‡] Department of Physics.
[⊗] Abstract published in *Advance ACS Abstracts,* July 1, 1994.

(1) Haigh, J.; Aylett, M. R. *Prog. Quantum Electron.* **1988**, *12*, 85.
(2) Chen, C. J.; Gilgen, H. H.; Osgood, R. M. *Opt. Lett.* **1985**, *10*, 173.
(3) (a) Jubber, M.; Wilson, J. I. B.; Davidson, J. L.; Fernie, P. A.; John, P. *Appl. Phys. Lett.* **1989**, *55*, 1477. (b) Jubber, M.; Wilson, J. I. B.; Davidson, J. L.; Fernie, P. A.; John, P. *Appl. Surf. Sci.* **1989**, *43*, 70. (c) Jubber, M.; Wilson, J. I. B.; Davidson, J. L.; John, P.; Roberts, P. G. *MRS Symp. Proc.* **1989**, *158*, 129. (d) Davidson, J. L.; John, P.; Jubber, M. G.; Milne, D. K.; Roberts, P. G.; Wilson, J. I. B. *Adv. Mater. Opt. Electron.* **1993**, *2*, 3.
(4) (a) Baum, T. H.; Jones, C. R. *App. Phys. Lett.* **1985**, *47*, 538. (b) Baum, T. H.; Jones, C. R. *J. Vac. Sci. Technol.* **1986**, *B4*, 1187. (c) Baum, T. H. *J. Electrochem. Soc.* **1987**, *134*, 216.
(5) (a) Banaszak Holl, M. M.; Seidler, P. F.; Kowalczyk, S. P.; McFeely, F. R. *Appl. Phys. Lett.* **1993**, *62*, 1475. (b) Banaszak Holl, M. M.; Seidler, P. F.; Kowalczyk, S. P.; McFeely, F. R. *Inorg. Chem.* **1994**, *33* (3), 510.
(6) Baum, T. H.; Marinero, E. E.; Jones, C. R. *Appl. Phys. Lett.* **1986**, *49*, 1213.
(7) Braichotte, D.; Van den Bergh, H. *Appl. Phys.* **1988**, *A45*, 337.
(8) Tamaki, A.; Kochi, J. K. *J. Organomet. Chem.* **1973**, *61*, 441.
(9) Van Leevwen, P. W. N.; Kaptein, R.; Huis, R.; Roobeck, C. F. *J. Organomet. Chem.* **1976**, *104*, C44.

0897-4756/94/2806-1712$04.50/0

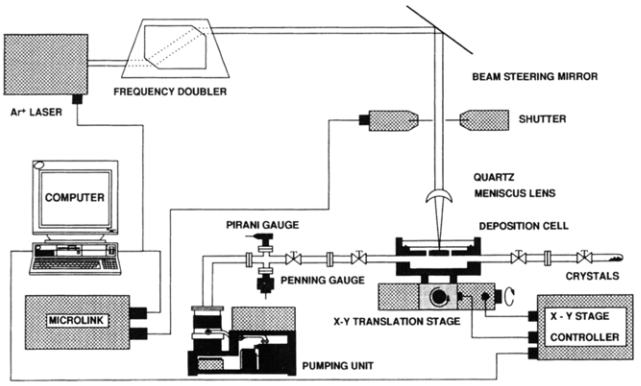

Figure 1. Schematic diagram of the apparatus used for the laser photochemical deposition of gold.

ion beam techniques. As a result, information on the incorporated molecular species in the tracks is limited. It is often extremely difficult to distinguish unequivocally molecular fragments from the bulk composition of the film by elemental ratios. For the elucidation of the complex processes occurring in photochemical systems, laser microprobe techniques[10] offer significant advantages in analyzing the deposited materials. Semiquantitative information on surface and near-surface composition can be obtained by ablation using a focused laser beam. Ablation at UV wavelengths permits molecular fragment ions to reach the detector intact. Furthermore, the replacement of charged particle beams by a laser pulse facilitates the analysis of poorly conducting materials without the limitations imposed by space charge effects. Variations in the pulse intensity of the probe laser and the absence of calibration standards for many materials, prevent accurate quantification of the data. Nevertheless, an insight into the chemical and physical processes governing the formation of a surface may be obtained from a semiquantitative analysis of the final composition. We report a laser ionization microprobe study of the composition of gold bearing tracks deposited by the argon ion laser photolysis at 257 nm of trimethylphosphine methylgold(I), $CH_3Au^IP(CH_3)_3$ (**1**), triethylphosphine methylgold(I), $CH_3Au^IP(C_2H_5)_3$ (**2**), and triethylphosphine ethylgold(I), $C_2H_5Au^IP(C_2H_5)_3$ (**3**). Our investigation underlines the importance of the chemical structure of the precursor in the laser photochemical deposition of high purity conducting gold.

Experimental Section

The compounds **1**−**3** were synthesized from $NaAuCl_4$ according to published methods[11] and purified by vacuum sublimation. Crystallisation from a diethyl ether solution yielded white crystalline solids. The compounds were characterized by ^1H NMR spectroscopy (Bruker WP 200SY) at 200.13 MHz. The compounds **1**−**3** possess a vapor pressure in the milliTorr range at 298 K and absorb wavelengths below 260 nm.[12,13] Thermal decomposition, established by DSC,[3] occurs in the range 60−80 °C.

The apparatus used for laser photochemical deposition is shown schematically in Figure 1. The frequency doubled output, at 257 nm, from a Coherent Innova Ar^+ laser was focused through a quartz window onto the substrate held within an evacuable stainless steel cell. The substrates were optically polished fused quartz and thermally grown SiO_2 (100 nm) on (100) crystalline silicon. The substrates were cleaned by washing in an untrasonic bath with successive aliquots of acetone, methanol and deionised water and were dried in a stream of oxygen free nitrogen. The purity of the organic solvents was better than 99.9%. The substrates were mounted onto a stainless steel heat sink within the cell. The distance from the inner surface of the window to the substrate was approximately 1 mm. The precursor vapor was admitted to the cell following evacuation to a base pressure below 10^{-6} mbar with a turbomolecular pump/rotary oil-pump combination. Second harmonic generation (Spectra-Physics, Model 395A) was accomplished using a single-pass intracavity mode configuration with a KDP doubling crystal which produced powers of 20−40 mW with a beam diameter of 2 mm. Laser powers were measured using a thermopile (Coherent) and were kept constant during the course of the experiment to within ±1 mW. The beam was focused by a quartz meniscus lens (f = 5 cm) to a diameter of approximately 20 μm at $1/e^2$ of the maximum intensity. Tracks were drawn by translating the cell under the focused laser beam with a high resolution (±0.1 μm) translation $x-y$ stage (Microcontrole) at speeds up to 200 μm s^{-1}. Deposition was monitored using an optical microscope focused onto the deposits through the cell window.

The morphology of the gold-bearing tracks was examined by Nomarski optical and scanning electron microscopy, SEM (Phillips Stereoscan). Track cross-sections were measured by scanning stylus profilometry (Dektak 3030) and $I-V$ characteristics by a micron-prober (Wentworth) connected to a Hewlett-Packard picoammeter. Gold contact pads, evaporated through a mask onto the end of the tracks, were probed with aluminum probe tips connected to the picoammeter terminals. Great care was taken to minimize the risk of contamination during the evaporation of the gold pads onto the ends of the tracks. The contact resistance between the probe tips and the gold pads, measured by placing both probe tips onto a single contact pad, made a negligible contribution to the measured resistance of the deposits. Elemental compositions and molecular inclusions within the deposits were measured by laser ionization microprobe analysis, LIMA (Cambridge Mass Spectrometry Ltd.). This technique used a single 3−5 ns pulse from a focused Nd:YAG laser operating at 266 nm to ablate and ionize a portion of the sample surface. The lateral spatial resulution was 1−2 μm in the focal zone. The composition of the resultant plasma was analysed by time of flight, TOF, mass spectrometry in either positive or negative ion mode. Accurate calibration of the mass scale was achieved by the observation of $[Cs(CsI)_n]^+$, n = 1−3 cluster ions from a thin CsI film deposited onto a section of the surface in contact with the deposits. The ablation/ionization chamber was constantly evacuated below 10^{-8} Torr. Samples were introduced from the laboratory via an evacuable loadlock. The sample was observed within the ablation/ionization chamber using an optical microscope which allowed the ablation laser beam to be accurately located onto the tracks. Ablation marks on the substrate were discernible after a single pulse, permitting mass spectra to be assigned to a specific point on the surface. Depth profiles of a sample were obtained by comparing the spectra arising from a successive series of laser pulses impinging at a fixed position on the sample.

Results and Discussion

Electrically conducting tracks were deposited onto fused quartz substrates from the 257 nm photolysis of compound **1**. Absorption coefficients and photolysis pathways have not been reported for the compounds **1**−**3** in the gas phase. Deposits exhibited a rippled morphology with a period corresponding to the wavelength of the incident radiation. This effect has been observed frequently in photolytic deposition from ad-

(10) Moenke-Blankenburg, L. *Laser Microanalysis*; John Wiley and Sons: New York, 1989.
(11) (a) Coates, G. E.; Parkin, C. *J. Chem. Soc.* **1962**, 3220. (b) Coates, G. E.; Parkin, C. *Ibid.* **1963**, 421. (c) Gregory, B. J.; Ingold, C. K. *J. Chem. Soc.* **1969**, *B* 276.
(12) Jubber, M. G. Ph.D. Thesis, 1991, Heriot-Watt University.
(13) Roberts, P. G. Ph.D. Thesis, 1993, Heriot-Watt University.

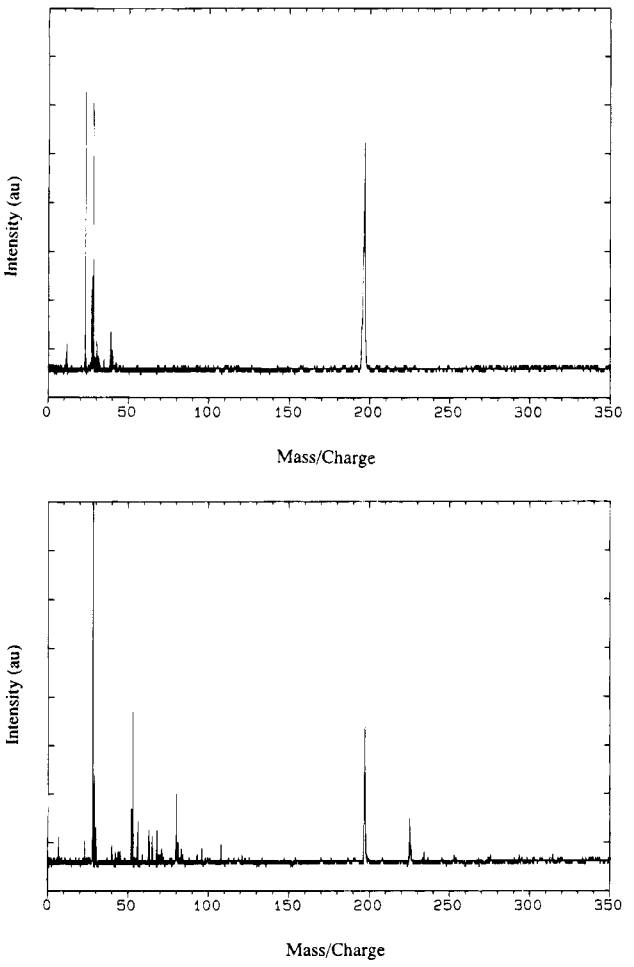

Figure 2. Laser ionization spectra, over the range m/z = 0–350, of (a) a track deposited upon SiO_2 from **1** (40 mW, 7.5 μm s^{-1}) and (b) a crystalline film of **1** deposited upon a silicon substrate. Contamination from Na, K, and Ca is observed at m/z = 23, m/z = 39, and m/z = 40, respectively. Depth profiles, obtained by successive laser pulses, demonstrated that these contaminants were located exclusively at the deposit surface.

sorbed precursors.[14] However, the tracks lacked the micron scale structural periodicity associated with those deposited from the same compounds by pyrolytic techniques.[3d] In the absence of a deposit, the substrate temperature within the focal spot, calculated according to the equations of Lax,[15] does not rise by more than 3.1 °C under laser irradiation at 40 mW. This is insufficient for thermal decomposition on an SiO_2 surface.[3,5] It is, therefore, reasonable to assume that deposition is initiated predominantly by photochemical decomposition. However, the presence of a thin gold film is likely to alter the thermal and optical properties of the surface within the focal spot. It is, consequently, impossible to exclude the possibility of a further temperature rise caused by an increase in optical absorption during film growth. Complete absorption of an incident laser power of 40 mW will yield a rise in temperature of 3.8 °C. However, the high thermal conductivity of gold relative to that of oxidized silicon is likely to compensate for such an effect by the conduction of heat through the deposit. Nevertheless, it has been reported[5] that gold films may be deposited from **1** and the related compounds $CH_3CH_2Au^IP(CH_3)$ and $CH_3CH_2Au^IP(CH_3)_3$ onto atomically clean copper and chromium surfaces at temperatures as low as 24 °C. It is, therefore, possible that thermal decomposition contributes to the deposition of tracks from the compounds **1**–**3** once photochemical nucleation has occurred. Since no deposition rates have been reported for the thermal CVD of gold from these compounds, it is difficult to estimate the extent of this contribution. Moreover, the possibility of a constantly changing surface during photochemical film growth would make the extrapolation of thermal CVD rates unreliable. Tracks with cross-sectional areas in the range 0.40–3.60 μm^2 were deposited at scan speeds ranging from 2 to 24.6 μm s^{-1}. Ohmic resistivities of 4.51 $\mu\Omega$ cm were measured for tracks deposited from **1** at 40 mW and a scanning speed of 7.5 μm s^{-1}. This is within a factor of 2 of the value for bulk gold (2.44 $\mu\Omega$ cm). In contrast, all of the tracks deposited from **2** and **3** under identical conditions were highly resistive. The I–V characteristics of the latter were nonlinear and exhibited hysteresis upon reducing the voltage from the terminal value. Thus changes in the nature of the precursor molecular radically altered the electrical properties of the resulting gold-bearing deposits.

Features of the microchemistry occurring at the interface of the substrate and the growing film were revealed by a LIMA investigation, using an ablation wavelength of 266 nm. Figures 2a–4a show the positive ion spectra of tracks deposited from compounds **1**–**3**, respectively. Gold was detected in all the tracks. The highest mass ion detected in tracks deposited from **1** is Au^+ at m/z = 197, while in tracks deposited from **2**, an additional peak was detected at m/z = 331 corresponding to the pseudo-molecular ion. In tracks deposited from **3** a peak was observed due to the fragment ion $[AuP(C_2H_5)_3]^+$ at m/z = 315. Possible sources for the signal at m/z = 225 include he $[AuSi]^+$ cluster ion, or alternatively, the $[C_2H_4Au]^+$ fragment ion, which has been observed in previous studies of the thermal dissociation of organogold complexes.[16] A close correspondence between the observed isotopic ratios and the calculated values for $[AuSi]^+$ supports the assignment of the latter signal to this ion. The desorption/ionization laser was focused onto the tracks to a spot diameter of approximately 1 μm and the point of ablation could be viewed using an in situ optical microscope. Away from the tracks, the observed fragmentation pattern was due solely to the substrate.

For comparison Figures 2b–4b show the spectra of **1**–**3** obtained from thin polycrystalline films of each compound, deposited onto an aluminum or silicon base by evaporation from a diethyl ether solution. The highest mass fragment ion derived *directly* from **1** occurred at m/z = 197 due to $[Au]^+$. The highest mass fragment ions derived from **2** and **3** occurred at m/z = 315 and 197 due to $[AuP(C_2H_5)_3]^+$ and $[Au]^+$, respectively.

Both the $[AuP(C_2H_5)_3]^+$ fragment ion and the Au^+ ion signal were detected throughout the whole volume of the tracks deposited from **3**. Upon depth profiling the track to the interface with the SiO_2 substrate, the ratio of the $[AuP(C_2H_5)_3]^+$ to Au^+ ion yield, $R = I(315)/I(197)$,

(14) Singmaster, K. A.; Houle, F. A.; Wilson, R. J. *J. Phys. Chem.* **1990**, *94*, 6864 and pertinent references therein.
(15) Lax, M. *J. Appl. Phys.* **1977**, *48* (9), 3919.
(16) (a) Comita, P. B.; Kodas, T. T. *Appl. Phys. Lett.* **1987**, *51*, (24) 2059. (b) Kodas, T. T.; Comita, P. B. *J. Appl. Phys.* **1989**, *65*, (6) 2513.

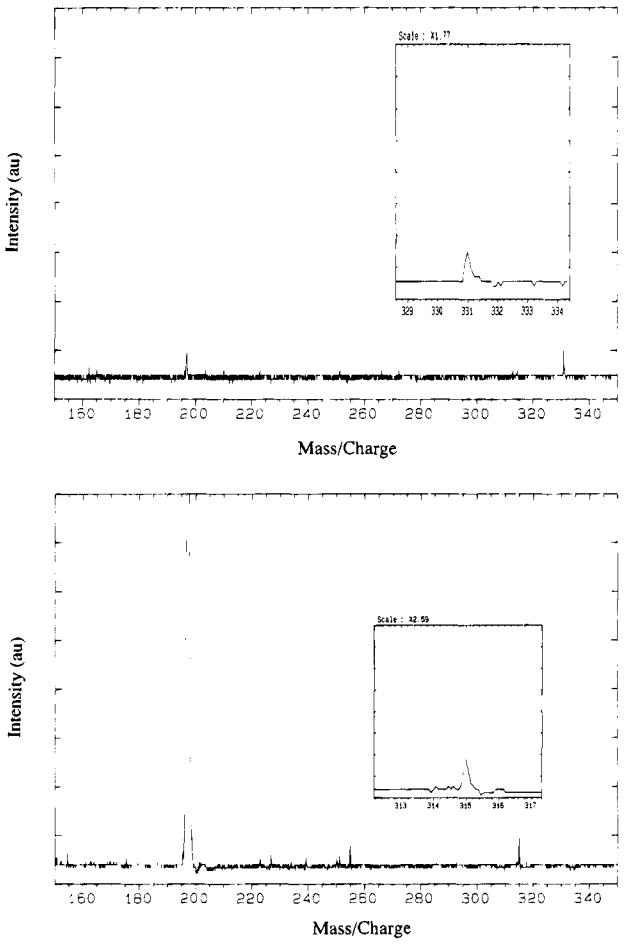

Figure 3. LIMA spectra, over the range m/z = 150–350, of (a) a track deposited from **2** (40 mW, 7.5 μm s^{-1}) and (b) a crystalline film of **2** deposited upon a silicon substrate. The inset of Figure 3a shows, on an expanded scale, the presence of a peak at m/z = 331 which is attributed to the pseudomolecular ion. The inset to Figure 3b shows, on an expanded scale, the presence of a peak at m/z = 315, corresponding to the $[AuPEt_3]^+$ ion.

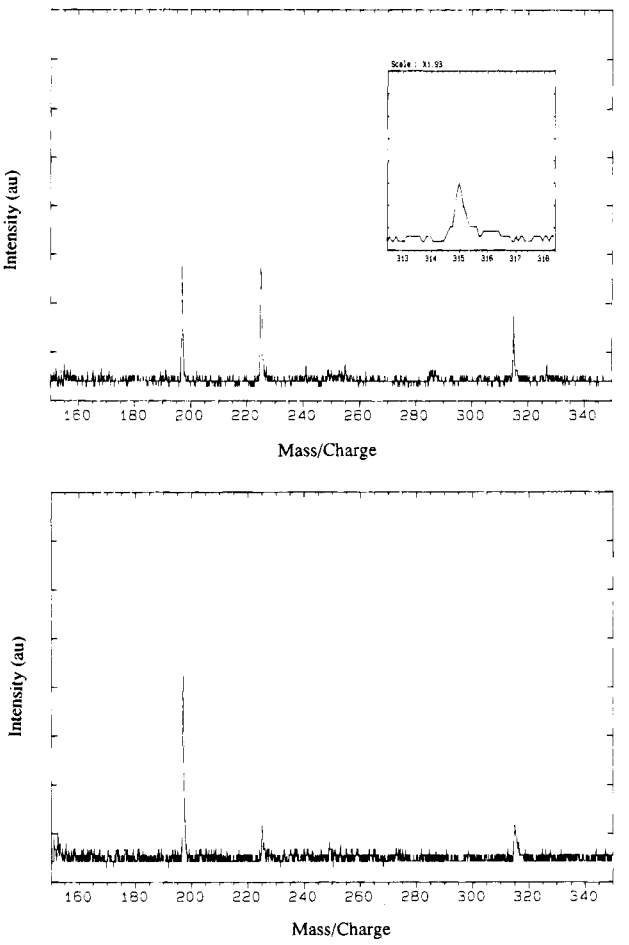

Figure 4. LIMA spectra, over the range m/z = 150–350, of (a) a track deposited from **3** (40 mW, 7.5 μm s^{-1}) and (b) a crystalline film of **3** upon an aluminum substrate.

varied with probe depth. Figure 5 shows the value of R with the number of consecutive laser shots. The highest value of R occurred at the track–substrate interface.

Tracks obtained from all three compounds were isochronally annealed in air at 50, 100, and 150 °C for the duration of 1 h. Those obtained from **1** underwent a increase in resistivity by at least 1 order of magnitude after annealing at 50 °C and were rendered highly resistive by annealing at or above 100 °C. The reduction in conductivity may result from thermal stresses induced within the tracks, caused by the large difference in the coefficient of thermal expansion between the substrate and deposit. The resistivity of tracks deposited from **2** and **3** were not altered by annealing.

The spectra of the tracks deposited from **1** and **2** remained unchanged following annealing at each of these temperatures. The spectra of tracks deposited from **3** following heating at 50 °C were unchanged compared with the original spectra. However, spectral changes were observed after annealing at higher temperatures. Figure 6 is representative of the spectra obtained from tracks deposited from **3** after heating at 100 °C. Notably the $[AuP(C_2H_5)_3]^+$ peak has disappeared. A dramatic increase in the relative abundance

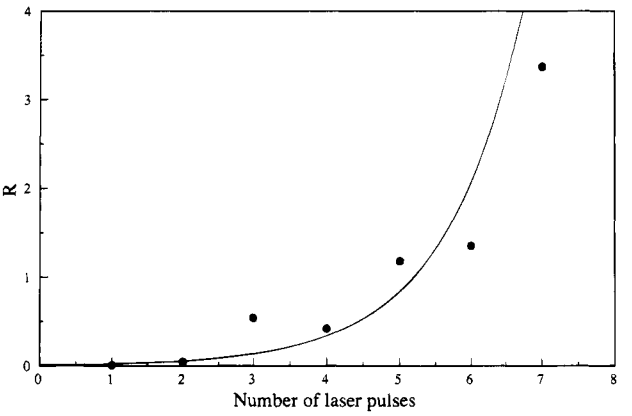

Figure 5. Variation of the $[AuPEt_3]^+$ to Au^+ ion yield R = $I(315)/I(197)$ ratio with the number of consecutive laser shots.

of the $[AuSi]^+$ cluster ion peak at m/z = 225 was also observed. The relative intensity of this peak increased near to the substrate. This result is not fully understood at present but may be associated with the interdiffusion of Au and Si/SiO_2. A similar phenomenon in which silicon rapidly diffuses through thin gold films at low temperatures has been reported.[17] The formation of a Au/Si alloy by interdiffusion could also account for the increase in resistivity which was observed after annealing the tracks deposited from **1**. However, the un-

(17) Hiraki, A. *Surf. Sci. Rep.* **1984**, *3*, 357.

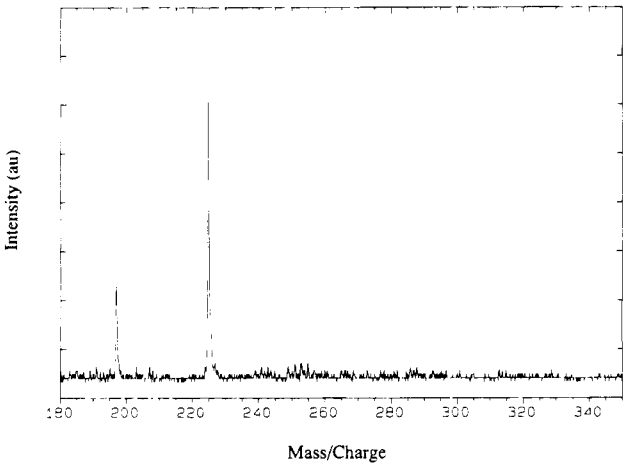

Figure 6. LIMA spectrum, over the range m/z = 180–350, of a track deposited from **3** (40 mW, 7.5 μm s^{-1}) after isothermal annealing at 100 °C. Assignment: Au^+ (m/z = 197); $[AuSi]^+$ (m/z = 225).

changed intensity of the AuSi peak after isochronal annealing does not support this explanation.

The effect of changes in the surface composition with film growth was investigated by comparing the spectra of **1** and **2** *adsorbed* from the gas phase upon Au and SiO_2, respectively. A clean SiO_2-coated Si wafer, half of which had been coated with ca. 1000 Å gold film by vacuum evaporation, was attached to an aluminum substrate. A polycrystalline layer of the organometallic complexes was formed on the aluminum substrate adjacent to the wafer by evaporation from a dilute solution in diethyl ether. The sample was subsequently placed in a vacuum chamber and evacuated to below 10^{-8} Torr so that the wafer was exposed to the vapor pressure of the compound at 25 °C. After 1 h the sample was transferred under vacuum from the loading chamber to the laser ionization chamber while remaining under vacuum. The coated and uncoated regions of the wafer surface were subject to successive pulses from the defocussed ablation laser. For comparison, identical wafers, also partly coated with gold, were exposed to the vapor pressures at 25 °C of $P(CH_3)_3$ and $P(C_2H_5)_3$ respectively and subsequently analyzed by LIMA under the same conditions.

The spectrum of the gold surface after exposure to **1** is shown in Figure 7a. A small, reproducible peak corresponding to the molecular ion at m/z = 288 was observed in addition to a stronger signal at m/z = 273 assigned to the $[AuP(CH_3)_3]^+$ fragment. A peak at m/z = 76 corresponding to $[P(CH_3)_3]^+$ was observed in conjunction with a series of peaks resulting from the dissociation of $P(CH_3)_3$. Peaks at m/z = 225 and m/z = 237 were observed which correspond to $[AuSi]^+$ and $[AuSiC]^+$, respectively. The presence of the molecular ion is evidence for a chemisorbed layer of the complex on the gold surface. The intensities of the signals at m/z = 273 and m/z = 288 were unchanged after pumping on the sample for 24 h. Exposure of the sample to air for the same period eliminated the molecular ion signal and substantially diminished the signal due to the $[AuP(CH_3)_3]^+$ fragment. No additional peaks were observed after exposure to air. These results suggest that the molecule is strongly chemisorbed onto the gold surface but that its reactivity upon exposure to air is comparable to that reported for **1** in the solid state.[11]

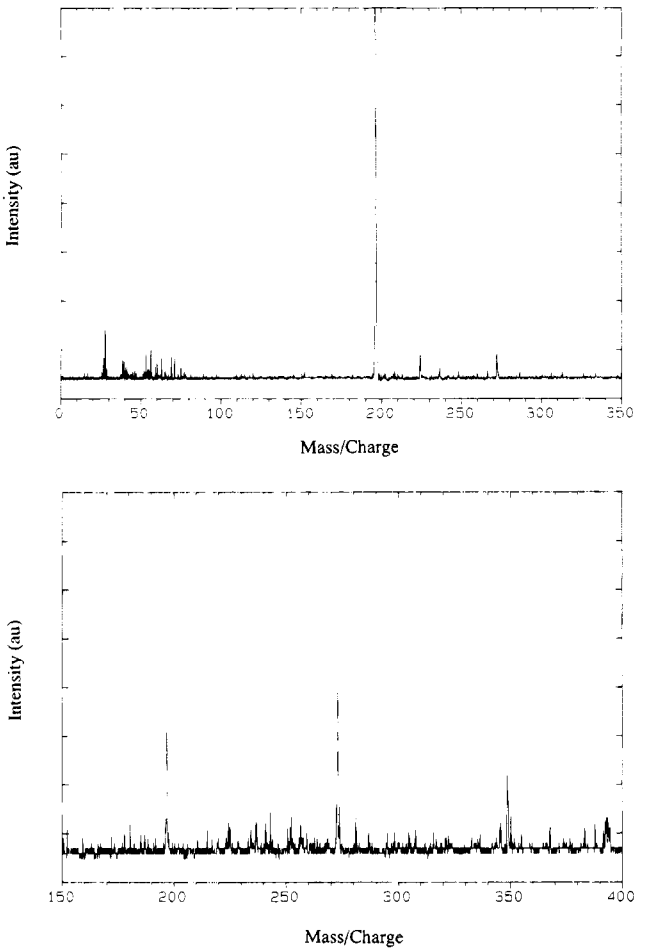

Figure 7. LIMA spectrum of an evaporated gold surface following exposure to the saturated vapour pressures at 295 K of (a) **1** and (b) PMe_3, over the ranges m/z = 0–350 and m/z = 150–400, respectively.

The $[AuP(CH_3)_3]^+$ fragment at m/z = 273 observed after exposure of the gold surface to **1** may result from dissociation of the parent molecule by the probe laser. However, it is also conceivable that free $P(CH_3)_3$ liberated from **1** and subsequently adsorbed onto the gold surface, may give rise to the same fragment ion following laser ablation. Figure 7b shows the spectrum obtained from the gold surface following the exposure of the wafer to $P(CH_3)_3$ at 25 °C. In addition to a peak due to the $[Au]^+$ ion, peaks occur at m/z = 273 and m/z = 349, corresponding to $[AuP(CH_3)_3]^+$ and $[Au\{P(CH_3)_3\}_2]^+$, respectively. The latter ion was invariably the less abundant. Both peak intensities were undiminished after evacuation for 24 h, while the former signal persisted, albeit with reduced signal strength, after 24 h of exposure to air. The results indicate, first, that a strong affinity exists between $P(CH_3)_3$ and a gold surface and second, that the adsorbate gives rise to $[AuP(CH_3)_3]^+$ fragment ions upon laser ionization. The same ion signal is observed in the spectrum of **1**, both in the crystalline form and when adsorbed onto gold from the gas phase. Since the photolytic decomposition of **1** liberates $P(CH_3)_3$, it is impossible to distinguish directly between $[AuP(CH_3)_3]^+$ fragment ions derived from the dissociation of the chemisorbed molecules of **1**

and those resulting from the chemisorption of unligatedP(CH_3)$_3$ onto the gold surface. The chemisorption of P(CH_3)$_3$ onto gold was not observed in previous X-ray photoelectron spectroscopy, XPS, investigations.[5b] This discrepancy may be explained by the different experimental conditions and analytical techniques which were employed. In particular, the gold surface was exposed to a much higher dose of P(CH_3)$_3$ in the present study.

In contrast to the strong ion signals resulting from the laser desorption of species chemisorbed onto the gold surface, analysis of the bare SiO_2 surface revealed relatively low intensities of fragment ions. After exposure of SiO_2 to **1** the [AuP(CH_3)$_3$]$^+$ signal was present, but the molecular ion was not observed. This observation also contrasts with the results of previous XPS investigations[5b] into the interaction of SiO_2 and **1**, where no evidence was found for adsorption from the gas phase at 25 °C. The detection, in the present study, of the [AuP(CH_3)$_3$]$^+$ ion suggests that the same ion produced from the gold surface might be partially derived from the parent molecule rather than entirely from free P(CH_3)$_3$. However, as illustrated in Figure 7a, the molecular ion was observed in very much lower abundance than the [AuP(CH_3)$_3$]$^+$ fragment, possibly as a result of dissociation of the parent molecule by the probe laser. This, coupled with the generally lower ion yield obtained from the SiO_2 surface than from the gold surface, might render the molecular ion signal below the detection limits of the instrument. A weak signal at m/z = 76 attributed to [P(CH_3)$_3$]$^+$ was also evident. Again, the signal strengths were unaffected by pumping upon the chamber for 24 h, whereas the peaks persisted with reduced intensities after exposure to air for the same period. Interestingly, the spectrum of SiO_2 exposed to P(CH_3)$_3$ did not exhibit a molecular ion at m/z = 76, or indeed any associated fragmentation pattern. Therefore, the [P(CH_3)$_3$]$^+$ ion observed in the spectrum of SiO_2 exposed to **1** was derived from either the parent molecule, or from fragmentation of the [AuP(CH_3)$_3$]$^+$ ion.

The molecular ion was not observed in the mass spectrum obtained after exposure of the gold surface to **2**, but a peak due to the [AuP(C_2H_5)$_3$]$^+$ was present. Therefore, it is impossible to rule out the dissociative chemisorption of **2** onto the gold surface. The molecular ion, together with a series of fragment ions, was detected in the spectrum obtained after the exposure of the gold surface to P(C_2H_5)$_3$. Moreover, the [AuP(C_2H_5)$_3$]$^+$ ion signal was also detected. This peak was also present in the spectra of **2**, obtained both from a polycrystalline film and when chemisorbed from the gas phase onto a gold surface. In the latter case the [AuP(C_2H_5)$_3$]$^+$ ion signal may arise from the photoionization of chemisorbed molecules of **2** and chemisorbed molecules of unligated P(C_2H_5)$_3$. Since these routes to the fragment ion are indistinguishable, it is impossible to establish the relative contribution of each to the [AuP(CH_3)$_3$]$^+$ ion signal observed after the exposure of the gold surface to **2**.

In neither of the spectra obtained, following the exposure of an SiO_2 substrate to **2** and P(C_2H_5)$_3$, respectively, were any fragment ions detected which might derive from these species. The spectra were essentially that of a clean substrate. This implies that if either compound is chemisorbed onto SiO_2 the surface coverage is below the detection limit of the mass spectrometer.

The above results reveal distinct trends in respect of the adsorption of compounds **1** and **2** onto gold and SiO_2 surfaces, respectively. Strong chemisorption onto gold is demonstrated by both compounds, with the ion yield from **1** being greater than that from **2**. This trend is mirrored in the behavior of P(CH_3)$_3$ and P(C_2H_5)$_3$. There is evidence for the nondissociative adsorption of **1** upon gold. Surface coverage of both complexes, as determined by the fragment ion yield, is lower upon SiO_2 than upon gold with that of **2** being below the detection limit of the instrument.

These results are particularly interesting in the light of the selective CVD of gold onto metal surfaces at ambient temperatures.[5] The high surface coverages with which compound **1** and **2** adsorb onto gold, as opposed to SiO_2, are consistent with the previous observation[5b] that the low-temperature decomposition of **1** and similar compounds on a gold surface is preceded by selective chemisorption. The spectral data shows that **1** and **2** strongly chemisorb to gold, but the detection of the molecular ion in the spectrum of **1** adsorbed onto a gold surface suggests that the subsequent dissociation of this compound may be slow. It is possible that the thermal dissociation of the adsorbed precursor is dependent upon a sufficiently long residence time and that such a condition is only satisfied by strong chemisorption. A detailed study of the adsorption isotherms and dissociation rates of trialkylphosphine alkylgold(I) compounds on various materials may confirm this hypothesis. A mechanism has been proposed for the thermal dissociation of **1** and the related compound $CH_3CH_2Au^IP(CH_3)_3$ on a gold surface.[5b] This was based, by analogy, upon previous mechanistic studies of the thermal dissociation of triphenylphosphine alkylgold(I) complexes in solution.[8] Initial cleavage of the Au−P bond, occuring via dissociative chemisorption onto a gold surface, was cited as the rate-determining step. The detection of LIMA, of $AuPR_3$ fragments, but not AuR'_3, suggests that the former species are the more stable. However, previous reports[5b] that the exposure of a gold surface to P(CH_3)$_3$ did not result in the detection of adsorbed P(CH_3)$_3$, albeit under different experimental conditions and analytical techniques, conflict with the results presented here. A strongly chemisorbed layer of PR_3 might be expected to obstruct the further adsorption of the precursor, but gold CVD from **1** was not retarded significantly by exposure to P(CH_3)$_3$ vapor.[5b] Further work is required to clarify the role of adsorbed PR_3 in the thermal CVD of gold from these complexes.

While the [AuP(C_2H_5)$_3$]$^+$ signal is absent from spectra of the tracks deposited from **3** upon annealing at 100 °C, the fragmentation pattern at lower mass remains unchanged. Molecules of **3** chemisorbed onto the surface of the tracks cannot be entirely responsible for the [AuP(C_2H_5)$_3$]$^+$ ion since upon depth profiling the abundance of this fragment increases near to the interface with the substrate. The results presented above suggest that if chemisorbed precursor molecules were responsible for the fragment then a higher abundance would be expected upon the surface than at the interface. The opposite trend is observed. Moreover, although the ion yields of **1** and **2** are greater when adsorbed upon gold than upon SiO_2, tracks deposited from these compounds

do not exhibit the corresponding $[AuPR_3]^+$ signals, although tracks deposited from **2** exhibits a weak signal due to the molecular ion. Furthermore, the mass spectra of all three precursor complexes exhibit a sequence of peaks derived from the dissociation of the ligated trialkylphosphine. This sequence is present neither in the original tracks nor after annealing. For these reasons the tracks deposited from **3** contain species other than discrete molecules of the precursor compound. The evidence suggest that trapped photolytic fragments, e.g., $AuP(C_2H_5)_3$ and $P(C_2H_5)_3$, contribute to the film impurities and that these neutral fragments are ionized during the LIMA analysis. From the experiments performed, it is impossible to distinguish between $[AuPR_3]^+$ ions derived from the photodissociation of the parent molecule and those derived from the chemisorption of unligated PR_3 to a gold surface.

As discussed above, it is difficult to estimate the extent of thermal contributions to the growth of the photochemically nucleated deposits. However, trapped molecular fragments have not been detected in gold films obtained by thermal CVD from trialkylphosphine alkylgold(I) precursors,[3,5] suggesting that the fragments described above derive from photochemical reactions. The increased abundance of trapped photolytic fragments of **3** near the interface between the track and the deposit are consistent with an increasing thermal contribution to the deposition reaction with deposit thickness.

The 257 nm photodissociation of **1** yields tracks with high electrical conductivities whereas those deposited under the same conditions from **2** or **3** are highly resistive. It is conceivable that the photolytically generated $[AuPR_3]$ or $[PR_3]$ fragments of the latter compounds are incorporated into the growing film, thereby creating occlusions and that the effect of these upon the material is to dramatically reduce the electrical conductivity compared to that of the bulk metal. It is also possible that the more volatile fragments derived from **1** escape from the reaction zone more readily, especially at the low surface temperatures associated with 257 nm laser irradiation. The absence of trapped photolytic fragments from the tracks deposited from **1** may also result from a larger thermal contribution to the dissociation of this compound. A greater thermal influence over the composition of tracks deposited from **1** than over those from **2** and **3** may also account for the lower resistivities observed in the former. Obstacles to the commercial application of laser assisted CVD include low deposition rates, and the difficulty of producing conducting tracks on thermally sensitive substrates.[18] These results raise the possibility of the photolytic nucleation of gold features by a fast "direct write" process, followed by low-temperature thermal CVD to produce highly conducting deposits.

Under certain conditions, laser-induced processes may proceed via two stages.[7] In many cases of metal deposition[1] upon an absorbing substrate the initial layer is formed from the photodissociation of the adsorbed precursor layer. As the thickness of the deposit increases, the laser power is gradually absorbed by the metal film, leading eventually to the predominance of higher film temperatures and the onset of photothermal deposition. Under a translating laser beam, this effect might lead to spatial inhomogeneities in composition arising from the differing rates and mechanisms of the competing photochemical and photothermal processes. This model explains qualitatively the enhanced yield of dissociation fragments at the film–substrate interface detected in the analyses described above. Following the photodissociation of the adsorbed molecular layers, the released PR_3 fragments are strongly chemisorbed onto the gold surfaces. The density of the growing film is reduced by the effect of this surface coverage and consequent incorporation of PR_3. The resulting conductivity is not improved at temperatures up to 150 °C, since the metallic layer is probably not consolidated, although the PR_3 fragments are released.

Conclusions

In summary, the photolysis of **1** at 257 nm yields high-purity gold tracks with conductivities within a factor of 2 of the bulk value. However, we have demonstrated that the production of high-purity electrically conducting gold tracks by photolytic LCVD is highly sensitive to the structure of the organogold precursor, even within a homologous series. Thus deposits obtained from triethylphosphine alkylgold(I) precursor complexes exhibit much higher resistivity values than those obtained from the $P(CH_3)_3$ derivative. Mass spectral data obtained by the laser ionization technique indicate that the precursors and the free PR_3 ligands adsorb more strongly to a gold surface than to a Si/SiO_2 surface. Furthermore, the affinity of the precursor for both gold and SiO_2 surfaces increases with the size of the PR_3 ligand. The evidence suggests that the incorporation of the precursor and/or various photolysis byproducts into the deposit is controlled by the volatility of the ligand and its absorptive properties on gold. Further evidence is provided by the removal of the contaminants by isothermal annealing above 100 °C. However, the resulting electrical conductivities are not improved. In conclusion, analysis by LIMA has provided an insight into the incorporation of photolysis byproducts which ultimately determine the composition and electrical conductivities of the metallic deposit. Further work is in progress to delineate the role of adsorbate photolysis and elucidate the complex steps leading ultimately to elemental gold.

Acknowledgment. We thank the UK SERC/MoD for financial support and SERC for a studentship (P.G.R.). We acknowledge Johnson-Matthey for the loan of $NaAuCl_4$ and Gerry Smith of Edinburgh Surface Analysis Technology for obtaining the LIMA spectra. We are indebted to Dr. David Milne for valuable discussions and to Iain Drummond for the construction of the experimental apparatus.

(18) Baum, T. H.; Comita, P. B. *Thin Solid Films* **1992**, *218*, 1–2, 80.